Journal of Molecular Structure 1336 (2025) 142107

Contents lists available at ScienceDirect

Journal of Molecular Structure

journal homepage: www.elsevier.com/locate/molstr

Carboxyl-functionalized bis(carbamoylcarboxylic) acid ligands as a novel alternative for hazardous metal ions removal by coagulation-flocculation

Jorge Guzmán-Rasillo [a], Adrián Ochoa-Terán [a,*], Eduardo A. López-Maldonado [b,*], Sergio Pérez-Sicairos [a], Balter Trujillo-Navarrete [a], Luis Miguel López-Martínez [c], José García-Elías [a], Paul A. Sandoval-Hernandez [a], Marisela Martínez Quiroz [d]

[a] Centro de Graduados e Investigación en Química, Tecnológico Nacional de México/IT Tijuana, Tijuana, B.C. México
[b] Faculty of Chemical Sciences and Engineering, Autonomous University of Baja California, 22424, Tijuana, B.C., Mexico
[c] Universidad Estatal de Sonora (UES), Hermosillo, Sonora, México
[d] CETYS Universidad, Tijuana, B. C., México

ARTICLE INFO

Keywords:
Carboxyl-functionalized
Carbamoylcarboxylic
Metal ions
Coagulation-flocculation
Zeta potential

ABSTRACT

In this work, a new series of carboxyl-functionalized bis(carbamoylcarboxylic) acid ligands (*bCCAs*) was synthesized to evaluate their performance as coagulant-flocculant agents. The interaction of these ligands with metal ions was evaluated in solution by UV-Vis spectroscopy in organic media finding 1:2 and 1:1 (metal:ligand) complexes. Zeta potential (pZ) analysis demonstrate the negative charge of these ligands at low pH, as well as the charge neutrality adding metal ions reaching the isoelectric point (IEP) due to the complexation in aqueous media. The *Log* K_a values (2.517 to 3.887) indicate a strong metal-ligand interaction in water. These new *bCCAs* demonstrate outstanding performance in the simultaneous removal of metal ions such as Ca^{2+}, Cd^{2+}, Cu^{2+}, Ni^{2+}, Pb^{2+} and Zn^{2+}, acting as both coagulant and flocculants in a coagulation-flocculation process, and showing excellent removal capacities (308 to 533 mg M^{n+}/g of L or 1.94 to 3.68 mol M^{n+}/mol of L), clarification kinetics (48.6 to 136.8 T%/h) and sedimentation ratios (96 to 156 mm/h). Comparing with the *bCCAs* type ligands previously studied, these carboxyl-functionalized analogues perform the fastest coagulation-flocculation process. These results indicate a high potential for effectively removing metal ions from industrial wastewater.

1. Introduction

Water is one of the most important natural resources on Earth, since it is not only essential for life existence, but it is also fundamental for the functioning of our societies. However, water scarcity has been a persistent problem throughout history. It is one of the main challenges because, throughout the 20th century, the demand for water increased at a rate twice as the population growth rate, and, as a consequence, a large number of the population are living in areas with water scarcity [1–3]. There is enough water to satisfy the demand of the entire population. Nevertheless, the water is distributed unevenly, contaminated, or wasted. This has led to the search for methods to treat water and mitigate the impact of scarcity. Water treatment methods have been developed throughout the history, but with the increase in water demand, it has been necessary to implement new and more efficient methods. Water treatment methods consist of the contaminants removal improving water physicochemical and organoleptic qualities, so that it becomes suitable for consumption or use in some processes [4–6].

Water treatment using the coagulation-flocculation method is a chemical method carried out before a physical separation process, such as filtration or decantation [7–9]. It is used to treat water contaminated with colloidal particles and consists of adding a coagulant agent that neutralizes the charges of these particles so they agglomerate and form larger particles called micro-flocs. Subsequently, a flocculation process follows adding a flocculant agent, the mixture is slightly stirred to facilitate the micro-flocs' agglomeration, the formation of larger particles and their settlement [10,11]. Then, the mixture is allowed to rest for a time, and a two-phase system is formed with a solid phase of sludge at the bottom, which contains all the removed contaminants, and a liquid phase or clarified water at the top. Finally, this system is separated by a physical method [11]. The coagulation-flocculation method has the advantages of simplicity, cost-effectiveness, the ability to remove

* Corresponding authors.
E-mail addresses: adrian.ochoa@tectijuana.edu.mx (A. Ochoa-Terán), elopez92@uabc.edu.mx (E.A. López-Maldonado).

https://doi.org/10.1016/j.molstruc.2025.142107
Received 9 August 2024; Received in revised form 4 February 2025; Accepted 18 March 2025
Available online 18 March 2025

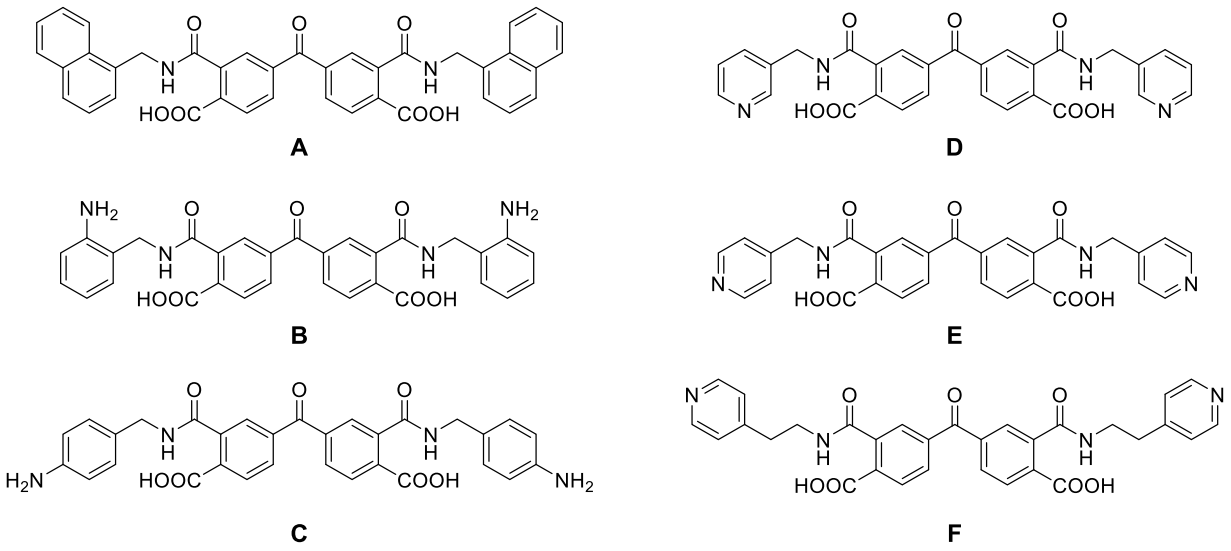

Fig. 1. Best performing functionalized *bCCAs* previously studied as coagulant-flocculant agents in wastewater treatment.

different types of particles, and improved filtration efficiency [12–14]. However, it also has the disadvantage of being a very slow process; contaminants are transferred to a sludge, which must be treated later and the use of chemical products is required [15–17].

The development of industry and human activities, such as the metal coating industry, batteries, pesticides, the mining industry, metal washing processes, the textile industry, metal smelters, petrochemicals, paper manufacturing, and electrolysis applications, had increased the presence of heavy metals in wastewater. Wastewater contaminated with metallic ions spreads up in the environment, compromising human health and different ecosystems. Heavy metals are not biodegradable, and the presence of these metals in wastewater results in severe health problems for living beings [18]. Heavy metals are elements with high atomic weight and density. These elements have multiple applications in different fields of human activity, which contribute to their environment distribution and raise potential effects on the health of living beings and the environment [16,19]. There are several factors that influence their toxicity, such as dose, exposure route, chemical species involved, as well as, the affected individual characteristics such as age, gender, genetics, and nutritional status. Because of their high toxicity, metal ions such as arsenic, cadmium, chromium, lead, and mercury are considered the highest-priority contaminants causing severe health problems. These metallic elements are considered systemic toxic agents that, although they are detected in trace amounts still dangerous [20,21]. Heavy metals can cause damage to the body's organs even with minimal exposure and are also classified as carcinogens [21,22].

In the treatment of wastewater containing heavy metals, coagulation consists in destabilizing metal ions by neutralizing the positive charges and keeping them separated using a chemical agent with an opposite charge [23,24]. At the same time, flocculation is the agglomeration of the resulting particles formed in the coagulation. Traditional coagulants are aluminum, ferrous sulfate, and ferric chloride, which are used to neutralize the charges of the ions [8,25]. Flocculation is the process in which particles join to form large agglomerates due to the action of coagulant-flocculant agents, such as poly aluminum chloride (PAC), polyacrylamide (PAM), poly ferric sulfate (PFS), and other flocculating macromolecules. Polyelectrolytes are the most practical flocculants, but the sludge resulting from the process is toxic. The most of coagulating-flocculating agents are non-natural and non-biodegradable [10,26,27]. These processes have several drawbacks, including the toxicity and health risks of inorganic coagulants, a large volume of sludge, selectivity for some metals, and inefficiency with emerging contaminants. Additionally, natural coagulants are ineffective, and it is challenging to scale up the process. Common metals targeted by this approach include Cu^{2+}, Pb^{2+}, and Ni^{2+} [11,18].

The design of easily synthesized compounds for metal ions detection and removal has attracted attention in the area of environmental chemistry, due to the biological and environmental importance of ions [23,28–30]. The bis(carbamoylcarboxylic) acid ligands have been studied as chelating agents for metal ions to achieve the formation of complexes in organic and aqueous medium [25,31,32]. The *N,N*-dibenzyl, *N,N*-dinaphthyl, and *N,N*-dinaphthylmethyl *bCCAs* can bind with Pb^{2+}, Cu^{2+}, and Hg^{2+} in a 1:1 ratio. Interestingly, the formed complexes with Pb^{2+} precipitate in water, achieving a removal efficiency of up to 95 % with an average removal capacity of 950 mg of Pb^{2+} per gram of ligand **A** (1.3 mol Pb^{2+} per mol of **A**) (Fig. 1). The clarification kinetic is 146.9 T%/h, and the sedimentation ratio is 27.5 mm/h [25]. Additionally, twelve aniline- and pyridine-functionalized *bCCAs* are capable to simultaneously remove seven metal ions (Cr^{3+}, Pb^{2+}, Cu^{2+}, Cd^{2+}, Ni^{2+}, Zn^{2+}, and Ca^{2+}) from water with good average removal efficiencies and capacities ranging from 124 to 937 mg of metal ions per gram of ligand [33]. Ligands **B**-**F** showed the best performance as coagulant-flocculant agents in removal of metal ions from water, particularly ligand **E** showed an 80.3 % average removal efficiency, a removal capacity of 937 mg of M^{n+}/g of **E** (7.33 mol of M^{n+}/mol of **E**), a clarification kinetic of 55.9 T%/h and a sedimentation ratio of 117.6 mm/h at the optimal dosage of 300 mg/L. These ligands have the characteristic that they act at the same time as a coagulant and flocculant agents in the cation removal process. It has been proposed that their ditopic nature and chelating properties induce to form coordination polymers that, as increase in weight and size, they separate from water [25,31].

Furthermore, chitosan grafted with *N*-benzyl *bCCA* performed the simultaneous removal of a mixture of cations with good efficiency (66 % to 99 %) [16,24], but a high dose of grafted polymer was required (1.12 to 1.15 g of M^{n+}/g of grafted chitosan). The performance parameters were improved grafting the chitosan with aniline and pyridine functionalized *bCCAs*, this grafted chitosan showed good removal efficiencies (73 % to 99 %) and excellent removal capacities of metal ions (43.5 to 50 g of M^{n+}/g of grafted chitosan) [34].

Based on the previous results obtained with *bCCAs* ligands, the interaction of new carboxyl-functionalized *bCCAs* with metal ions was analyzed by UV-vis spectroscopy and pZ to evaluate their complexation properties. Also, a micro-Jars test was developed to stablish their metal ions removal capacities and potential as coagulant-flocculant agents. It was expected that the additional carboxylic groups would enhance the

strength of the interaction and improve their performance in the coagulation-flocculation process.

2. Experimental

2.1. Instruments

The reagents and solvents used were commercially available and were not further purified. NMR spectra were recorded on a Bruker Avance 400 spectrometer in DMSO-d_6 at a probe temperature of around 23°C, using TMS as the internal standard. UV-Vis absorption spectra were measured with a Perkin Elmer Lambda 365 UV-Visible spectrophotometer, employing a 1 cm optical pass quartz cell. Zeta potential analysis was conducted using a Meinsberger Zeta Stabino instrument and a porcelain cuvette. Inductively coupled plasma optical emission spectroscopy (ICP-OES) analysis was performed with a Perkin Elmer Optima 8300. Fourier transform infrared spectroscopy spectra were recorded using a Perkin FTIR Spectrum Two spectrophotometer in the 400–4000 cm^{-1} frequency range.

2.2. General procedure for the synthesis of carbamoylcarboxylic acids

Benzophenone-3,3′,4,4′-tetracarboxylic dianhydride (200 mg, 0.62 mmol) was dissolved in 50 mL of dry acetonitrile (ACN) in a single-neck round-bottom flask. The solution was stirred at 0°C under an argon atmosphere for 10 min. Following this, 2.2 molar equivalents of the corresponding primary amine, previously dissolved in 5 mL of dry ACN, was added, and the reaction mixture was continually stirred for 8 h at room temperature. After this time, the solvent was removed under reduced pressure. The resulting solid was washed with ACN (2 × 25 mL) and with diethyl ether (3 × 25 mL). Subsequently, the solid was dried at room temperature to obtain a pure solid product [31].

4,4′-carbonylbis(2-((2-carboxyethyl)carbamoyl)benzoic) acid (3a). Pale yellow viscous liquid, 279.8 mg, 0.56 mmol, 89 % yield. FTIR: 3478, 2925, 1695, 1625, 1275, 1234 cm^{-1}. ^{1}H NMR (400 MHz, DMSO-d_6): δ 8.44 (s, 1H), 8.25 (d, J = 8.1 Hz, 1H), 7.88 (dd, J = 8.1, 2.0 Hz, 1H), 7.69 (s, 2H), 3.01 (t, J = 6.8 Hz, 2H), 2.58 (t, J = 6.8 Hz, 2H). ^{13}C NMR (101 MHz, DMSO-d_6): δ 172.41, 167.80, 167.58, 138.79, 138.32, 131.52, 35.34, 31.95, 31.14.

4,4′-carbonylbis(2-((4-carboxybuthyl)carbamoyl)benzoic) acid (3b). Yellow viscous liquid, 279.1 mg, 0.50 mmol, 80.8 % yield. FTIR: 3482, 2937, 1698, 1654, 1604, 1270, 1237 cm^{-1}. ^{1}H NMR (400 MHz, DMSO-d_6): δ 8.53 (d, J = 2.0 Hz, 2H), 8.34 (d, J = 8.1 Hz, 2H), 7.86 (dd, J = 8.1, 2.0 Hz, 2H), 2.76 (m, 2H), 2.25 (d, J = 13.1 Hz, 2H), 2.08 (m, 2H), 1.55 (p, J = 3.8 Hz, 10H). ^{13}C NMR (101 MHz, DMSO-d_6): δ 138.31,135.54, 134.37, 133.49, 131.27,39.06, 33.84, 31.14, 27.11, 21.92

4,4′-carbonylbis(2-((6-carboxyhexyl)carbamoyl)benzoic) acid (3c). Yellow solid, 344.1 mg, 0.56 mmol, 90.5 % yield. Mp 115-117°C. FTIR: 3467, 2930, 1702, 1652, 1604, 1277, 1239 cm^{-1}. ^{1}H NMR (400 MHz, DMSO-d_6): δ 8.53 (d, J = 2.0 Hz, 2H), 8.34 (d, J = 8.1 Hz, 2H), 7.87 (dd, J = 8.1, 2.0 Hz, 2H), 2.78 (t, J = 7.5 Hz, 2H), 2.21 (t, J = 7.3 Hz, 2H), 2.08 (s, 1H), 1.51 (dtd, J = 14.2, 11.0, 9.1, 5.6 Hz, 5H). ^{13}C NMR (101 MHz, DMSO-d_6): δ 174.91, 167.59, 139.02, 138.32, 135.54, 134.40, 133.52, 131.28, 39.32, 33.99, 28.42, 27.30, 25.92.

4,4′-carbonylbis(2-((7-carboxyheptyl)carbamoyl)benzoic) acid (3d). Pale yellow solid, 310.6 mg, 0.48 mmol 78.2 % yield. Mp 120-122°C. FTIR: 2952, 1681, 1628, 1610, 1290, 1250 cm^{-1}. NMR ^{1}H (400 MHz, DMSO-d_6): 8.53 (d, J = 2.0 Hz, 2H), 8.34 (d, J = 8.1 Hz, 2H), 7.87 (dd, J = 8.1, 2.0 Hz, 2H), 2.74 (m, 2H), 2.20 (t, J = 7.4 Hz, 4H), 2.08 (d, J = 5.9 Hz, 4H), 1.58 (m, 10H). NMR ^{13}C (101 MHz, DMSO-d_6): δ 195.17, 174.93, 167.61, 167.55, 139.00, 138.33, 135.52, 134.40, 133.51, 131.29, 39.34, 34.11, 28.78, 27.42, 26.08.

4,4′-carbonylbis(2-((3-carboxyphenyl)carbamoyl)benzoic) acid (3e). Pale yellow solid, 367.7 mg, 0.61 mmol, 96.3 % yield. Mp 213-215°C. FTIR: 3477, 2927, 1696, 1658, 1602, 1267, 1239 cm^{-1}. ^{1}H NMR (400 MHz, DMSO-d_6): δ 8.06 (d, J = 1.8 Hz, 2H), 7.95 (dd, J = 7.9, 1.8 Hz, 2H), 7.85 (d, J = 7.9 Hz, 2H), 7.20 (t, J = 1.6 Hz, 2H), 7.12 (m, 4H), 6.79 (dt, J = 6.7, 2.5 Hz,2), 3.39 (q, J = 7.0 Hz, 4H), 1.09 (t, J = 7.0 Hz, 6H). ^{13}C NMR (101 MHz, DMSO-d_6): δ 193.89, 168.74, 168.29, 167.87, 148.85, 138.31, 137.77, 132.76, 132.59, 131.83, 130.24, 129.36, 129.23, 118.71, 117.44, 115.17, 65.37.

4,4′-carbonylbis(2-((4-carboxyphenyl)carbamoyl)benzoic) acid (3f). Pale yellow solid, 362.7mg, 0.61 mmol, 98.0 % yiled. Mp 215-217°C. FTIR: 3456, 2936, 1683, 1649, 1602, 1284, 1240 cm^{-1}. NMR ^{1}H (400 MHz, DMSO-d_6): δ 8.04 (d, J = 1.8 Hz, 2H), 7.96 (dd, J = 7.9, 1.8 Hz, 2H), 7.83 (d, J = 7.9 Hz, 2H), 7.62 (m, 4H), 6.56 (m, 4H). RMN ^{13}C (101 MHz, DMSO-d_6): δ 168.78, 167.94, 167.89, 153.33, 138.31, 137.73, 132.67, 131.67, 130.11, 129.10, 117.46, 113.09.

4,4′-carbonylbis(2-((4-carboxybenzyl)carbamoyl)benzoic) acid (3g). Pale yellow solid, 380.8 mg, 0.61 mmol, 98.2 % yield. Mp 314-316°C. FT-IR: 3347, 2959, 1682, 1625, 1608, 1292, 1255 cm^{-1}. ^{1}H NMR (400 MHz, DMSO-d_6): δ 8.52 (d, J = 2.0 Hz, 2H), 8.32 (d, J = 8.1 Hz, 2H), 7.99 (dd, J = 8.3, 1.8 Hz, 4H), 7.87 (dd, J = 8.1, 2.0 Hz, 2H), 7.58 (d, 4H), 4.14 (s, 4H), 3.39 (q, J = 7.0 Hz, 1H), 2.08 (d, J = 5.6 Hz, 6H), 2.07 (s, 1H), 1.09 (t, J = 7.0 Hz, 1H). ^{13}C NMR (101 MHz, DMSO-d_6): δ 195.13, 167.55, 139.18, 138.32, 134.23, 137.34, 131.33, 132.59, 130.00, 129.35, 42.48, 31.14.

4,4′-carbonylbis(2-((4-carboxyphenylethyl)carbamoyl)benzoic) acid (3h). Pale yellow solid, 401.5 mg, 0.61 mmol, 96.5 % yield. Mp 312-314°C. FTIR: 3465, 2930, 1702, 1649, 1602, 1275, 1237 cm^{-1}. ^{1}H NMR (400 MHz, DMSO-d_6): δ 8.13 (s, 4H), 8.04 (d, J = 1.7 Hz, 2H), 7.93 (m, 4H), 7.84 (d, J = 7.9 Hz, 2H), 7.40 (m, 4H), 3.07 (td, J = 8.6, 6.8, 3.9 Hz, 4H), 2.99 (m, 4H). ^{13}C NMR (101 MHz, DMSO-d_6): δ 168.74, 167.86, 167.60, 143.05, 138.30, 137.36, 132.72, 132.61, 130.16, 129.80, 129.39, 33.31.

4,4′-carbonylbis(2-(hexylcarbamoyl)benzoic acid (3i). Yellow solid, 251 mg, 0.48 mmol, 77.3 %. Mp 120-122°C. ^{1}H NMR (400 MHz, DMSO-d_6): δ 8.53 (d, J = 2.0 Hz, 2H), 8.34 (d, J = 8.1 Hz, 1H), 7.86 (dd, J = 8.1, 2.0 Hz, 2H), 2.22 (d, J = 5.2 Hz, 4H), 1.55 (d, J = 3.4 Hz, 1H), 1.54 (s, 4H), 1.52 (s, 4H), 1.37 (s, 10H). ^{13}C NMR (101 MHz, DMSO-d_6): δ 138.31, 135.54, 134.37, 133.49, 131.27, 39.06, 33.84, 31.14, 27.11, 21.92.

4,4′-carbonylbis(2-(benzylcarbamoyl)benzoic acid (3j). White solid, 289 mg, 0.57 mmol, 91.9 % yield. Mp 156-158°C. ^{1}H NMR (400 MHz, DMSO-d_6): δ 8.54 (d, J = 2.1 Hz, 2H), 8.35 (d, J = 7.9 Hz, 2H), 7.93 (m, 2H), 7.43 (d, J = 7.9 Hz, 4H), 7.38 (d, J = 7.9, 4H), 7.30 (m, 2H), 3.96 (s, 4H). ^{13}C NMR (101 MHz, DMSO-d_6): δ 194.7, 167.3, 167.2, 138.6, 137.8, 133.9, 132.9, 130.8, 128.5, 128.3, 127.8, 43.3.

2.3. Study of the interaction of carboxyl-functionalized bCCAs with metal ions by UV-Vis spectroscopy

The metal complexation studies were performed using stock solutions at 1 × 10^{-5} M of each *bCCA* prepared by dissolving the corresponding amount of each ligand in acetonitrile HPLC grade. Stock solutions of $Cu(NO_3)_2$, $Pb(NO_3)_2$, $Ca(NO_3)_2$, $Cd(NO_3)_2$, $Zn(NO_3)_2$, and $Ni(NO3)_2$ were each prepared at a concentration of 1 × 10^{-2} M. Next, 3 mL of the ligand stock solution was added to a quartz cuvette, and then successive 3 μL aliquots of the salt stock solution were added to achieve the desired concentration range. The resulting solutions were stirred for 3 min, and their spectra were recorded. Throughout the measurements, the absorption spectrum was consistently found to be unchanged over time [20,25,26,33].

2.4. Zeta potential (ζ) = f (pH) trends for carboxyl-functionalized bCCAs

The surface charge properties of the *bCCAs* were determined by obtaining their zeta potential profiles at room temperature in a porcelain cuvette. The Zeta potential of the *bCCAs* (0.1 % w/v) was measured over a pH range of 2-11 by adjusting the pH of the solutions with 0.1 M HCl and 0.1 M NaOH while keeping the sample concentration constant [8,

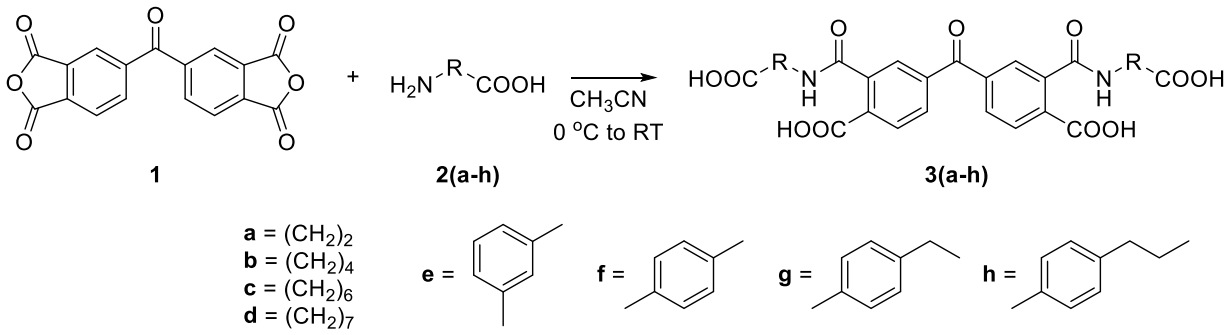

Scheme 1. Preparation of carboxyl-functionalized *bCCAs* **3a-3h**.

27].

2.5. Study of the interaction of carboxyl-functionalized bCCAs with metal ions by pZ

The effect of different metal cations (Cu^{2+}, Ca^{2+}, Ni^{2+}, Cd^{2+}, Pb^{2+}, and Zn^{2+}) on the pZ variation of carbamoylcarboxylic acids was examined in aqueous solutions at pH 4.6. The carbamoylcarboxylic acids were prepared as 0.1 % w/v stock solutions in ultrapure (MilliQ) water. Separate 0.16 M stock solutions of each metal ion (in the form of nitrate salts) were also prepared. A 10 mL initial volume of each compound solution was titrated with successive 0.02 mL additions of the cation solutions, and the resulting zeta potential was measured [33,35].

2.6. Metal ions removal efficiencies with carboxyl-functionalized bCCAs

The micro-Jar test was conducted to assess the coagulation-flocculation process [8]. A model wastewater solution was prepared by dissolving the metallic nitrate salts in 1000 mL of ultrapure water. The tests were performed in 20 mL vials filled with 5 mL of the model wastewater. Progressive additions of 1, 2, 3, 4, and 5 mL of each *bCCA* solution were made. Water was added to reach 10 mL final solutions at 300, 600, 900, 1200 y 1500 mg/L, respectively, and a final metal ions concentration of Cu^{2+} (54.8 mg/L), Ca^{2+} (55.3 mg/L), Ni^{2+} (47.5 mg/L), Cd^{2+} (39.5 mg/L), Pb^{2+} (51.7 mg/L) and Zn^{2+} (39 mg/L). The solution contained metal ions with a final concentration of 288.4 mg/L at pH 4.6. Each mixture was stirred for 2 min and then left to settle for another 2 min. Then, the mixture was filtered to measure the metal ion concentration in the supernatant after the treatment. The analysis was

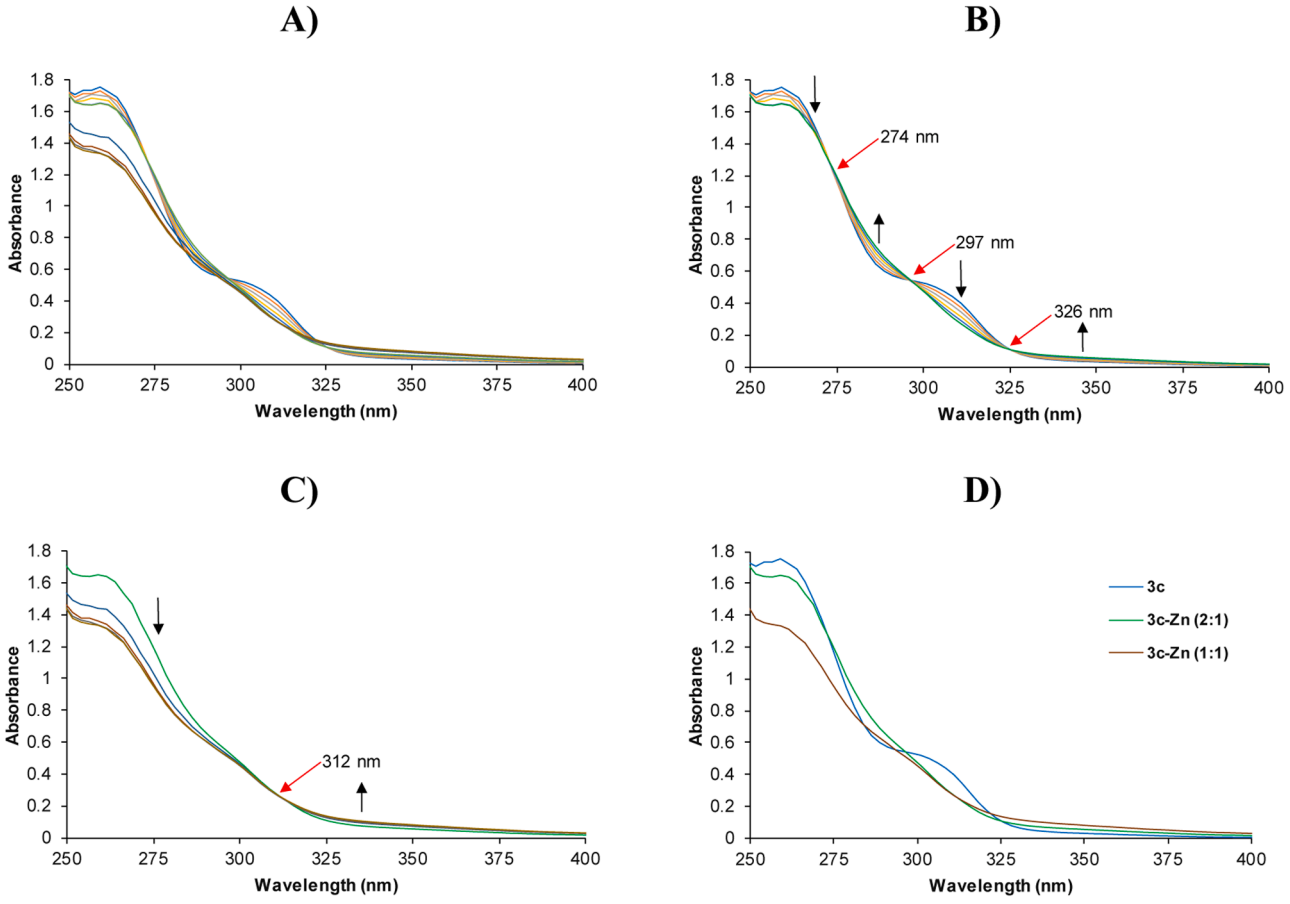

Fig. 2. A) UV-Vis spectra obtained in the titration of **3c** [1 × 10^{-5} M] with $Zn(NO_3)_2$ in acetonitrile. B) Spectra obtained in the titration from 0 to 0.5 molar equivalents. C) Spectra obtained in the titration from 0.5 to 1.0 molar equivalents. D) UV-Vis spectra for **3c,** **3c**-Zn (2:1) and **3c**-Zn (1:1).

done in axial mode, and the wavelengths for 327.39 nm -Cu^{2+}, 317.93 nm -Ca^{2+}, 267.71 nm -Cr^{3+}, 231.60 nm -Ni^{2+}, 228.80 nm -Cd^{2+}, 220.35 nm -Pb^{2+}, and 206.20 nm-Zn^{2+}. To ensure accuracy, all samples were analyzed three times [33].

2.7. Metal ions separation rates with carboxyl-functionalized bCCAs

The instability phenomenon was examined by measuring changes in transmittance and backscattering every 25 s over 1 h. This was carried out from the bottom to the top of the sample during the coagulation-flocculation process using a TURBISCAN LAB Expert instrument [27,35]. In the experiments, 10 mL of a *bCCA* solution at a concentration of 600 mg/L and pH 4.6 were combined with 10 mL of the cations solution to make a total volume of 20 mL. The sample was shaken for 1 min prior to analysis.

2.8. SEM analysis of recovered solids from a model wastewater treatment

The flocculated complex was separated using a filter membrane, dried in a convection oven, dispersed in ethanol, and then transferred to a microscopy support for observation [27]. The particulate with removed metal complex underwent analysis using a scanning electron microscope (Vega3, Tescan) equipped with secondary and backscattered electron detectors (BSE).

3. Results and discussion

3.1. Synthesis and physicochemical characterization

The synthesis of new carboxyl-functionalized *bCCAs* was done reacting benzophenone-3,3′,4,4′-tetracarboxylic dianhydride (**1**) with several alkyl **(2a-2d)** and aryl (**2e-2h**) amino acids in acetonitrile. This resulted in eight new carboxyl-functionalized *bCCAs* (**3a-3h**) obtained in high yield (90 to 99 %) and purity (Scheme 1) [31,32].

Compounds **3a-3h** were characterized by Nuclear Magnetic Resonance (^{1}H and ^{13}C NMR) and Infrared Spectroscopy (FTIR). The FTIR spectra for the eight carboxyl-functionalized *bCCAs* show similar vibrations due to they have the same core structure and functional groups [30]. The N-H stretching band is observed in the interval 3347 to 3482 cm^{-1}, a characteristic wide band from 2100 to 3700 cm^{-1} is observed for the O-H vibration as well as in the range of 1630 to 1740 cm^{-1} the overlapped vibration bands corresponding to the carbonyl groups. Additional vibrations are identified at 1602-1610 cm^{-1}, 1267-1292 cm^{-1} and 1234-1255 cm^{-1} intervals corresponding to C=C, C-N and C-O functional groups, respectively (see Table S1). The ^{1}H NMR spectra obtained in DMSO-d_6 show three doublet signals for the benzophenone core hydrogens at around 8.50, 8.25 and 7.97 ppm. The spectra of compounds with *N*-carboxyalkyl substituents (**3a-3d**) show two triplet signals at around 2.80 and 2.20 ppm which correspond to the methylene groups attached to nitrogen and carbonyl groups, respectively. The full assignment of the ^{1}H NMR signals for all compounds is provided in Tables S2 and S3. In the ^{13}C NMR spectra for all compounds are observed the characteristic signals at around 194 ppm assigned to the ketone carbonyl and two signals around 168 ppm assigned to the carbamoylcarboxylic functionality (amide and carboxylic carbonyls), but also there is observed a signal at 174 ppm (**3a-3d**) or 169 ppm (**3e-3h**) which corresponds to the carboxylic carbonyl at the *N*-substituent. The full assignment of the ^{13}C NMR signals for all compounds is provided in Table S4.

3.2. Study of the interaction of carboxyl-functionalized bCCAs with cations by UV-Vis spectroscopy

The electronic absorption spectroscopy method described in the experimental section was used to analyze the interaction between carboxyl-functionalized carbamoylcarboxylic acids **3(a-h)** and various

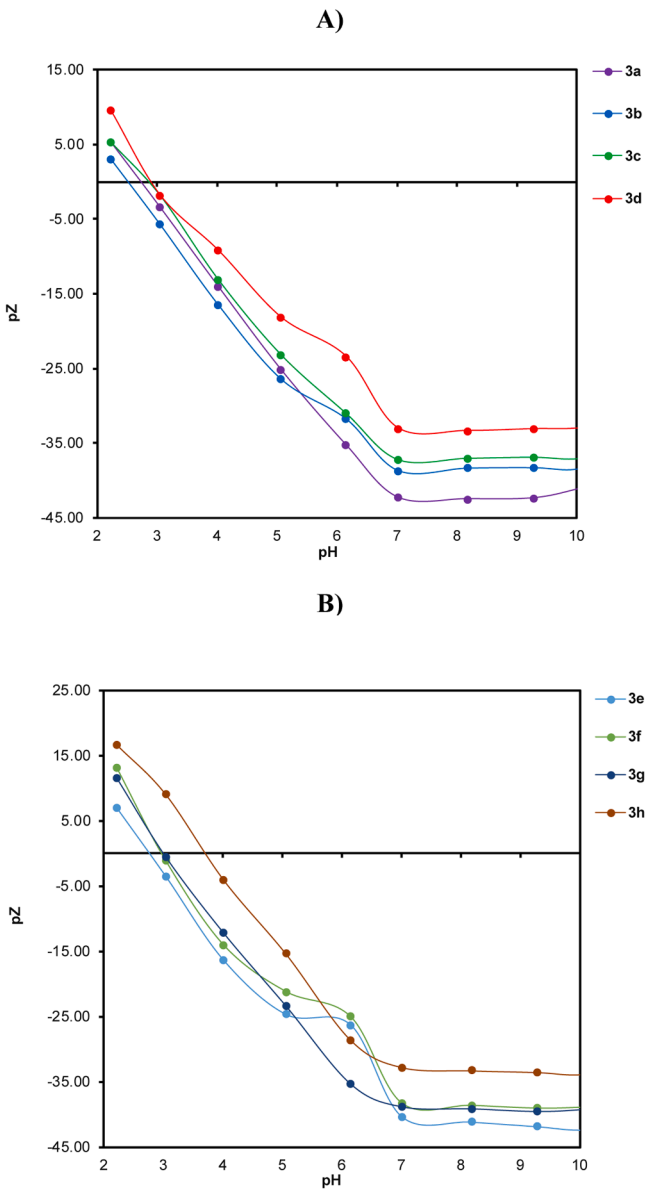

Fig. 3. pZ profiles as a function of pH for carboxyl-functionalized *bCCAs* **3a-3d** (A) and **3e-3h** (B) at 0.1 % w/v.

metal ions such as Ca^{2+}, Cd^{2+}, Cu^{2+}, Ni^{2+}, Pb^{2+}, and Zn^{2+} [25,31]. Fig. 2 shows the UV-Vis spectra of **3c** obtained by titration with Zn $(NO_3)_2$ in acetonitrile. The increased cation amount causes noticeable effects in the electronic transitions at 250 to 325 nm. Interestingly, the course of the titration clearly shows at least two different chemical species in equilibrium, from 0 to 0.5 molar equivalents of cation added to the solution three isosbestic points are observed at 274, 297, and 326 nm, indicating the formation of a coordination complex with 1:2 (metal: ligand) stoichiometry [31,33]. Then, there is a hypochromic change in the band by the addition of 0.5 to 1 molar equivalents of cation and it is observed a different isosbestic point at 312 nm. No significant change is observed in the absorption band beyond this amount of metal ion, suggesting the formation of a complex with a 1:1 (metal:ligand) stoichiometry. In general, compounds **3a-3d** form 1:2 metal-ligand complexes at low metal ion concentration, but at higher concentration predominant the 1:1 metal-ligand complexes (Figs. S1 to S23). The 1:1 metal-ligand stoichiometry suggests the formation of coordination polymers as occurs with other studied *bCCAs*. On the contrary, the titration of compounds **3e-3h** with metal ions does not show significant

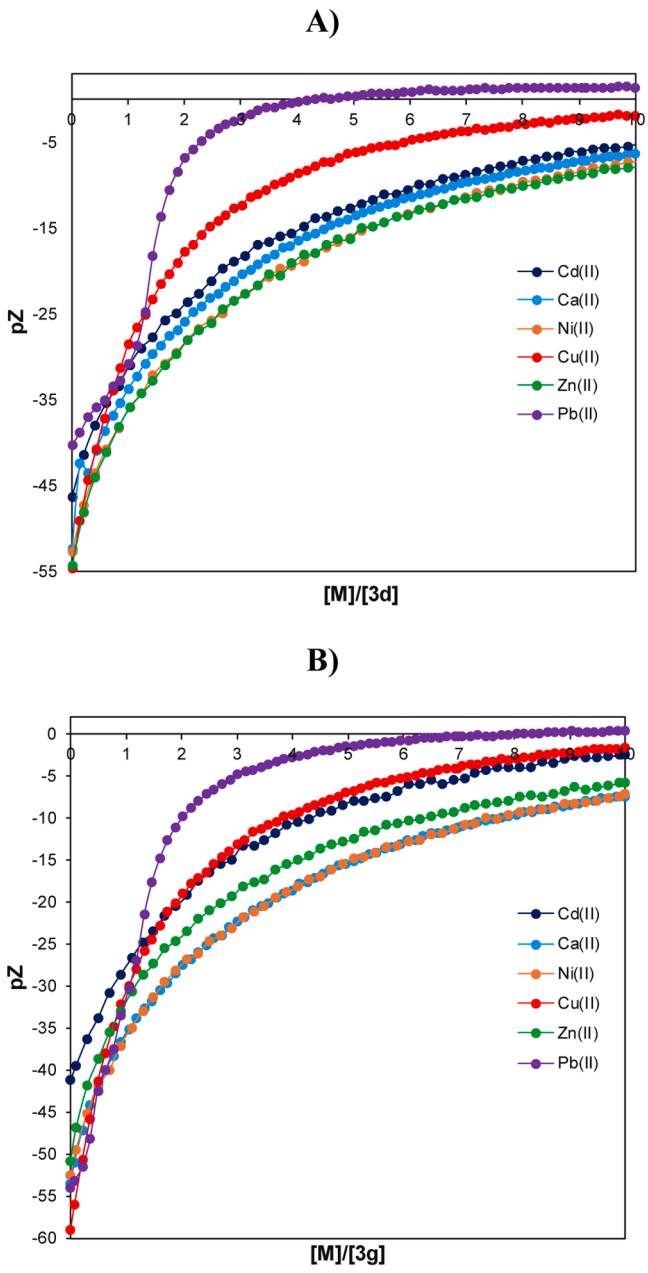

Fig. 4. pZ profiles obtained by titration of carboxyl-functionalized *bCCAs* **3d** (A) and **3g** (B) at 0.1 % w/v.

changes in the absorption bands, even at higher amounts of metal ion.

3.3. Zeta potential (pZ) vs pH profiles for carboxyl-functionalized bCCAs

The pH effect on the pZ of compounds **3a-3h** was examined at a pH range from 2 to 10. Fig. 3A and B illustrate the charge density changes of compounds with *N*-carboxyalkyl **3a-3d** (derived from alkyl amino acids) and *N*-carboxyaryl substituents **3e-3h** (derived from aromatic amino acids), respectively. The profiles of pZ = f (pH) for compounds **3a-3d** show a positive charge density (3-10 mV) at pH 2.2, the isoelectric points (IEPs) are in the range 2.5 to 2.9, reaching a minimum pZ of -42, -38, -37 and -33 mV at pH= 7, respectively (Fig. 3A). As it can be seen, the pZ limit increases as the alkyl chain of the substituent increases. Likewise, the profiles of pZ= f (pH) for compounds **3e-3h** show a positive charge density (7-17 mV) at pH 2.2, the IEPs are located at 2.75 to 3.7, reaching a minimum pZ of -41, -39, -39 and -33 mV at pH= 7, respectively (Fig. 3B). All these compounds have anionic character at low pH and their pZ limits are similar. Also, the IEPs of these carboxyl-functionalized *bCCAs* are similar to those found in the aniline- and pyridine-functionalized *bCCAs* previously reported, but their zeta potential limits are, in general, more positive [33]. The compounds exhibit a negative charge density at low pH, which is desirable for their use in the removal of metal ions through a coagulation-flocculation process.

Table 1
Association constants (*Log* K_a) for metallic complexes derived from carboxyl-functionalized *bCCAs* **3a-3h** and metal ions calculated from ζ profiles.

	Metal ion					
Ligand	Ca^{2+}	Cd^{2+}	Cu^{2+}	Ni^{2+}	Zn^{2+}	Pb^{2+}
3a	2.752 (23)	2.580(9)	2.810(6)	2.810 (21)	2.695 (18)	ND
3b	2.932 (30)	3.116 (32)	3.240 (42)	2.804 (28)	2.799 (38)	ND
3c	2.900 (31)	3.356 (58)	3.887 (96)	3.075 (32)	2.705 (12)	ND
3d	2.648 (20)	2.560 (12)	2.947(7)	2.517 (15)	2.577 (17)	ND
3e	2.928 (13)	3.195 (25)	3.128 (12)	2.676 (11)	3.109 (23)	3.470 (40)
3f	3.096 (68)	3.190 (33)	3.216 (14)	2.996 (56)	2.804 (28)	ND
3g	2.575 (15)	2.550(5)	2.943 (10)	2.536 (14)	2.695 (18)	3.038 (35)
3h	2.928 (10)	2.764(6)	2.987 (16)	2.879(5)	3.008 (19)	ND

ND= not determined.

3.4. Study of the interaction of carboxyl-functionalized bCCAs with metal ions analyzed by pZ

The interaction of ligands **3a-3h** with metal ions such as Pb^{2+}, Cu^{2+}, Ca^{2+}, Ni^{2+}, Zn^{2+}, and Cd^{2+} was evaluated in an aqueous solution at pH 4.6. This pH was chosen because at pH 4.6, the ligands have significant negative charge density (pH>IEP). In the experiments, the ligand solutions were prepared at 0.1 % (w/v) and were titrated with successive aliquots of metal ion solutions at 1.6×10^{-1} M until they reached 10 molar equivalents of the metal ion. The pZ profiles obtained from the titrations show an outstanding response with Pb^{2+} with all ligands reaching the IEP or going beyond showing an electropositive character at different molar equivalents (1.5 to 7.0), indicating a high affinity towards this metal ion, but variable depending on the ligand structure (Figs. 4 and S24 to S29) [34]. Interestingly, sigmoidal profiles are observed with Pb^{2+} instead of the typical asymptotic profiles obtained with the other ions; two complexation stages are observed with Pb^{2+}, which suggests a different complexation fashion as the concentration of metal ion increases (Figs. S31 and S32). This behavior was also observed in the titrations by UV-Vis in organic solvent. Also, some ligands such as **3b, 3c**, and **3f** reach the IEP with Cu^{2+} and Cd^{2+} at higher molar equivalents than Pb^{2+}, and in the titration of ligand **3h**, the IEP is reached with all the metal ions. Finally, there is a general response trend in the order $Pb^{2+} >> Cu^{2+} > Cd^{2+} > Zn^{2+} \approx Ca^{2+} \approx Ni^{2+}$.

Thordarson's non-linear 1:1 model was employed to calculate the association constants (*Log* K_a) for metallic complexes formed with the eight ligands and six metal ions in an aqueous environment using the ζ profiles [20,25,36]. Table 1 shows that the association constants are in the range of 10^2 to 10^3 M^{-1}, which are high values for an L-M^{n+} interaction in water. The *Log* K_a for most of the L-Pb^{2+} complexes could not be determined due to the pZ profiles not fitting with this model because of the abrupt change observed in the pZ caused by a strong interaction or a probable different complexes stoichiometry [33]. In general, ligands **3b, 3c** and **3f** have the higher *Log* K_a values and therefore the higher affinity toward metal ions. Also, it is observed that higher K_a were obtained for complexes with these carboxyl-functionalized *bCCAs* and

Table 2
Efficiency in the removal of metal ions with carboxyl-functionalized *bCCAs* at 300 mg/L and pH= 4.6.

Ligand	Removal efficiency (%)						Removal average	mg M^{n+}/ g of L	mol M^{n+} / mol of L
	Ca^{2+}	Cd^{2+}	Cu^{2+}	Ni^{2+}	Pb^{2+}	Zn^{2+}			
3a	24	68	50	48	98	49	56	533	3.23
3b	31	68	45	49	98	48	57	539	3.68
3c	30	61	26	44	95	43	50	473	3.48
3d	25	66	17	42	98	43	48	456	3.35
3e	17	16	28	15	94	14	31	308	1.94
3f	18	32	19	24	93	22	35	340	2.14
3g	24	46	21	34	94	32	42	401	2.87
3h	28	55	25	41	95	39	47	450	3.48

Ca^{2+}, Zn^{2+} and Cd^{2+} compared to the aniline- or pyridine-functionalized *bCCAs*, which may result in an improvement of the removal capacity of these metal ions.

3.5. Metal ions removal efficiencies with carboxyl-functionalized bCCAs

The ability of ligands **3a-3h** to act as coagulant-flocculant agents in

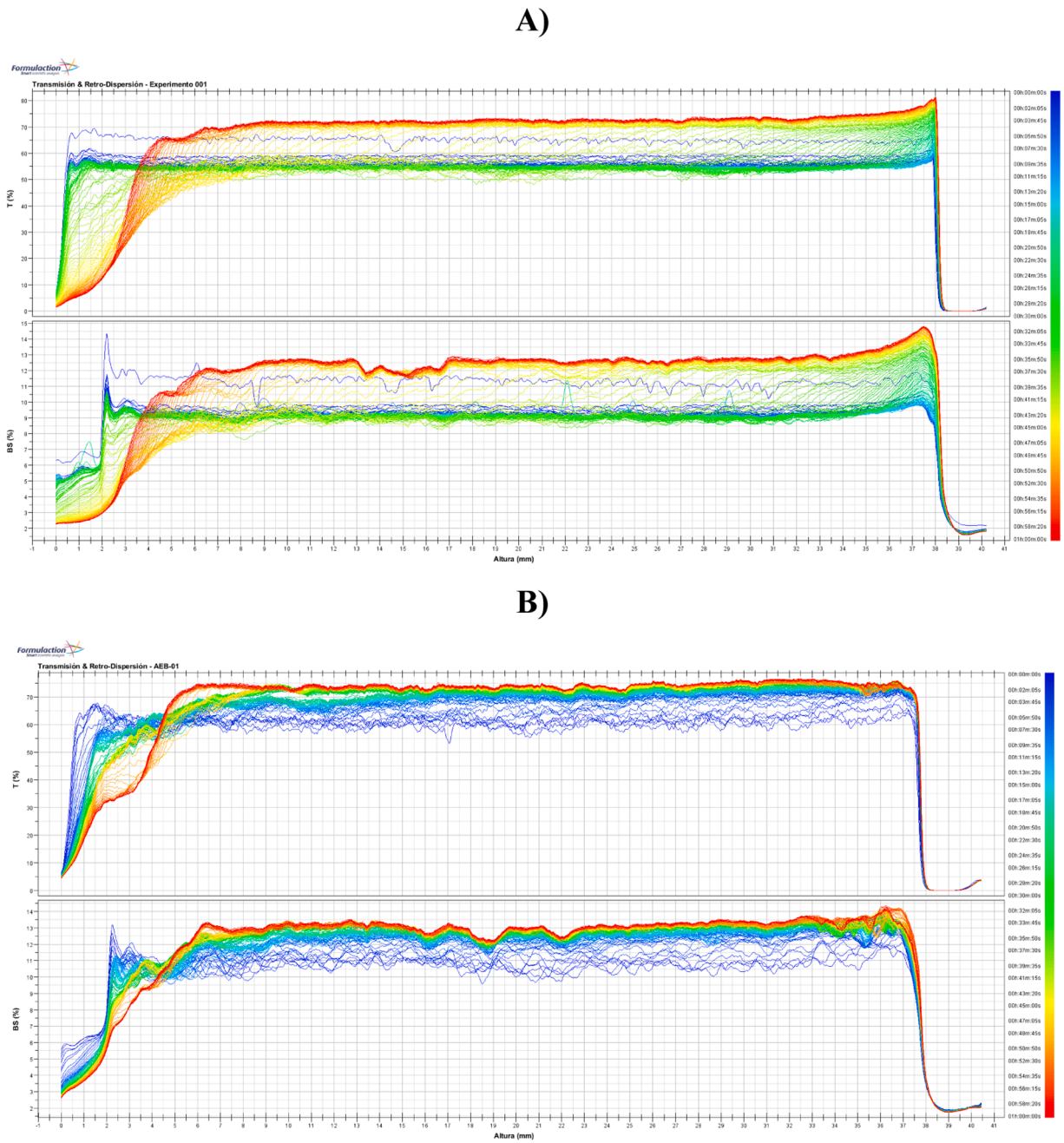

Fig. 5. ΔT(%) and ΔBS(%) trends of simulated wastewater treated with **3b** (A) and **3h** (B) at 300 mg/L and pH= 4.6.

treatment of a model wastewater with metal ions such as Cu^{2+} (54.8 ppm, 0.86 mmol/L), Ca^{2+} (55.3 ppm, 1.38 mmol/L), Ni^{2+} (47.5 ppm, 0.81 mmol/L), Cd^{2+} (39.5 ppm, 0.3514 mmol/L), Pb^{2+} (51.7 ppm, 0.25 mmol/L) and Zn^{2+} (39.6 ppm) frequently present in industrial effluents was tested by a micro-Jars test [8]. The metal ion solution was treated with the ligands **3a-3h** at 300, 600, 900, 1200 and 1500 mg/L in order to evaluate their removal performance and determine the optimal doses. The quantification of metallic content in the treated model wastewater by ICP-OES spectroscopy showed that at 300 mg/L (0.46 to 0.60 mmol/L) of ligands **3d, 3f** and **3h**, and at 600 mg/L (0.92 to 1.20 mmol/L) of ligands **3a, 3b, 3c, 3e** and **3g** were achieved the maximum metal ions removal, at higher concentrations it is observed a re-dispersion and stabilization of the flocs (see Tables S5 to S11). In order to compare the performance among these carboxyl-functionalized *bCCAs* and with previously studied aniline- and pyridine-functionalized *bCCAs* in wastewater treatment, a dose of 300 mg/L of ligand was selected for further experiments.

As shown in Table 2, all ligands showed the highest removal of Pb^{2+}, which is related to the high affinity of this ligands towards this metal ion, even in the presence of a molar excess of the other cations. In general, these ligands have a good metallic removal capacity (308 to 533 mg M^{n+}/g of ligand or 1.94 to 3.68 mol M^{n+}/mol of ligand) and it is observed a better performance with ligands containing *N*-carboxyalkyl substituents (**3a-3d**) with average removal efficiencies in the range of 48-56 % compared to 31-47 % for the ligands containing *N*-carboxyaryl substituents (**3e-3h**). Interestingly, as the length of the *N*-carboxyalkyl substituent increases from two to four methylenes, there is a slight increase in the efficiency and removal capacity and then it is observed a decrease with six and seven methylenes, indicating that the distance of the terminal carboxylic group has an important influence on the complexation and separation process of metal ions. The lowest efficiencies and removal capacities were obtained with ligands **3e** and **3f**, which have an aromatic ring directly attached to the amide group, but the efficiency and removal capacity increase with the ligands with one and two methylenes between the amide and the aromatic ring. In fact, ligand **3h** has a performance similar to **3c**. These results indicate that the steric factor also influences the performance of these ligands because the complexation process between the ligands and metal ions is less effective. Another important aspect of the removal performance of these ligands is the high removal of Ca^{2+} achieved compared to most of aniline- or pyridyl-functionalized analogues [33]. Based on the mass of removed Ca^{2+}, the removal efficiency is in the range of 17 to 31 %, but in terms of moles removed, its removal is comparable or even higher than the other metal ions. For example, the total molar removal capacity of **3b** is 3.68 mol of M^{n+}/mol of **3b**, but specifically for Ca^{2+} is 0.79 mol/mol of **3b** and for Pb^{2+} is 0.45 mol/mol of **3b**, under the experimental conditions employed. As it is well known, the carboxylate group has a great affinity towards Ca^{2+} ions which explains the removal enhancement obtained with these ligands containing several carboxylate groups (see Table S12). Based on their molar removal capacities, it is clear that ligands **3b, 3c,** and **3h** have the best removal performance.

3.6. Metal ions separation rates with carboxyl-functionalized bCCAs

The interaction of ligands **3a-3h** with metal ions leads to an instability phenomenon, which was determined by analyzing changes in transmittance (T) and backscattering (BS) profiles over time and across the sample. Using the TURBISCAN LAB instrument software, the clarification kinetics, sedimentation rate, and Turbiscan® Stability Index (TSI) were measured in a model wastewater treatment with each ligand [25–27]. The charge density and the hydrophilic or hydrophobic nature of these metallic complexes affect the destabilization process that determines the separation of metal ions through the coagulation-flocculation process [27,34].

Fig. 5 illustrates the transmittance and backscattering delta trends during the coagulation-flocculation process of simulated wastewater using ligands **3b** and **3h**. Figs. S32 to S40 show the profiles for the rest of the carboxyl-functionalized *bCCAs* and for the *N,N*-dihexyl *bCCA* **3i** and *N,N*-dibenzyl *bCCA* **3j** for comparative purposes. Ligand **3b** shows the highest removal capacity among the *N*-carboxyalkyl analogs, while among the *N*-carboxyaryl analogs is **3h**. The instability caused by each ligand is assessed by examining the percentage change in temperature (ΔT %) and in sample length (ΔBS %) at different points along the sample (top, bottom, and middle) [27]. Changes at the ends indicate local particle migration, while changes in the middle indicate overall particle size variation [20].

Table 3
Critical performance parameters in the coagulation-flocculation process with ligands **3a-3h** at 300 mg/L and pH= 4.6.

Ligand	Clarification kinetics (T %/h)	Sedimentation ratio (mm/h)	Removal capacity (mg M^{n+}/g)	TSI at 60 min	Phenomenon
3a	136.8	126	533	23.8	Coagulation-flocculation
3b	94.8*	6*	539	34.6	Coagulation-flocculation
3c	51.8	120	473	21.3	Coagulation-flocculation
3d	65.4	135	456	25.9	Coagulation-flocculation
3e	72.6	150	308	21.3	Coagulation-flocculation
3f	79.0	132	340	20.7	Coagulation-flocculation
3g	48.6	96	401	17.9	Coagulation-flocculation
3h	97.5	156	450	17.8	Coagulation-flocculation

* This is an estimated value due to the atypical behavior observed with this ligand.

The destabilization phenomenon seen with all ligands **3a-3h** corresponds to the coagulation-flocculation process, as indicated by the changes in ΔT(%) and ΔBS(%) in the central part of the samples (Table 3). TURBISCAN profiles show changes in light transmittance through the sample as a function of time or position along the sample. This allows to observe the evolution of the stability and structure of the dispersion. Based on this, it is notice that the structure of these three main regions are different for ligands **3b** and **3h** compared to non-carboxylated ligands **3i** and **3j** (Figs. S39 and S40). The profile of ligand **3i** behaves slow fluctuations in T % and BS % during the first 40 min, which is associated with the slowness colloids formation or insoluble metal complexes between the ligand **3i** and metal ions. Conversely, this phenomenon is observed in the profile of ligand **3b**, wherein, in the first minutes, the changes in T % decrease, and an abrupt increase occurs in BS %, remaining up to 25 min, which may be associated with the constant formation of insoluble complexes **3b**-M^{n+}, which continuously form aggregates.

The T % and BS % profiles observed with ligand **3j** have a similar behavior to the observed with ligand **3i**, there are only differences in the time domain of each stage, the constant period with minimum fluctuations in the sample is shorter (20 min) and it finally reaches a higher level of T % and BS %, indicating that the insoluble metal complexes formed are faster in sedimentation and achieving a greater speed of aggregation and clarification. These trends agree with the TSI profiles noted below. The chemical structure and the type of functional groups in these ligands determine complexation, aggregation processes, and floc formation. These factors translate into differences in the performance of these ligands for treating water with metal ions.

The clarification kinetics values obtained with most of carboxyl-functionalized *bCCAs* such as **3a, 3b, 3d, 3e, 3f** and **3h** are superior to those obtained with aniline- or pyridine-functionalized ligands, for example ligands **D** and **E** show clarification kinetics of 50.23 and 55.99 T

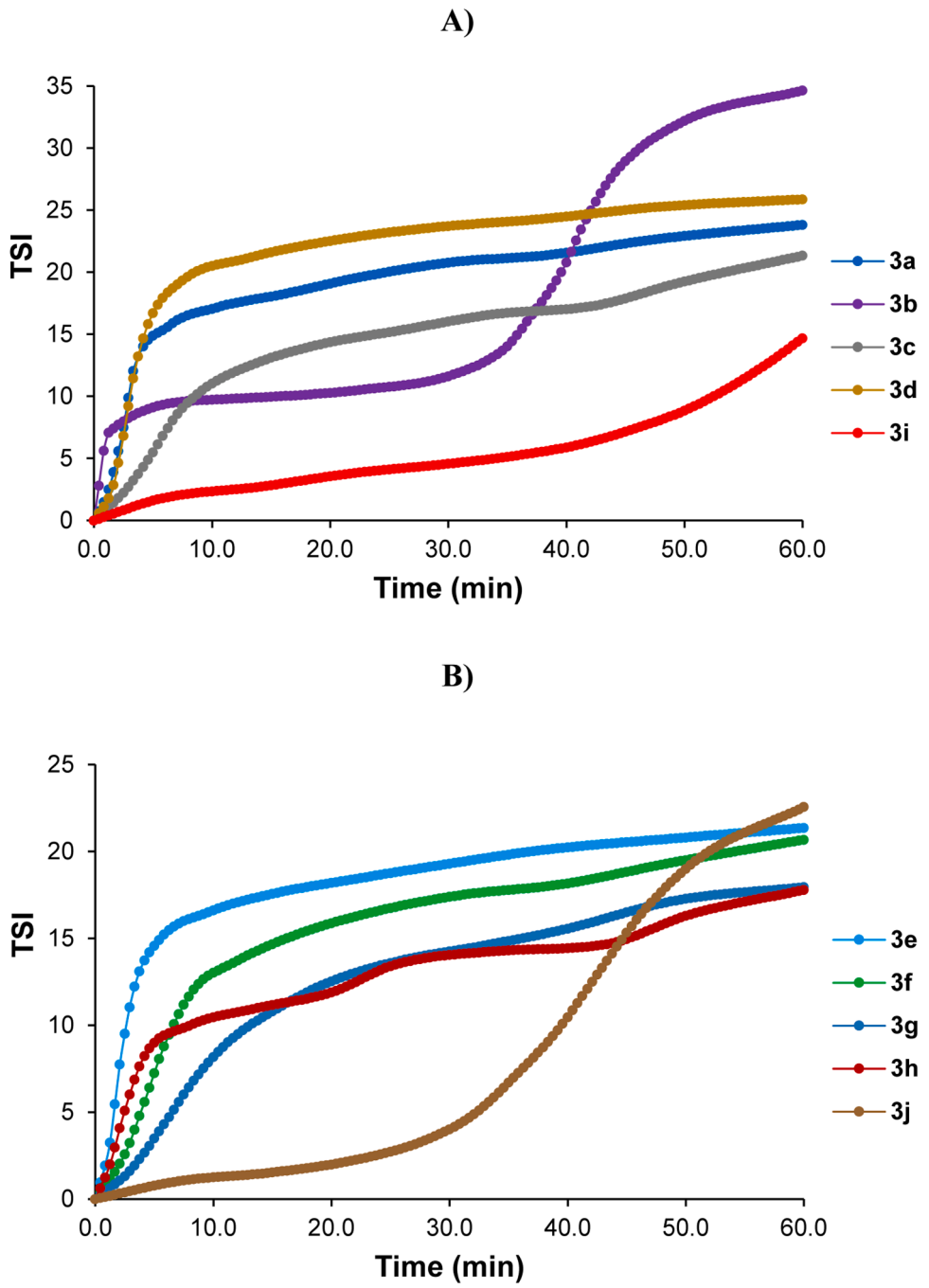

Fig. 6. TSI trends as a function of time until 60 min for A) *N*-carboxyalkyl *bCCAs* (**3a-3d**) and *N,N*-dihexyl *bCCA* **3i**, and B) *N*-carboxaryl *bCCAs* (**3e-3h**) and *N,N*-dibenzyl *bCCA* **3j**.

%/h, respectively, while ligands **3a** and **3h** have 136.8 and 97.5 T %/h, respectively (Table 3). Regarding the sedimentation ratio, the values previously reported for ligands **E** and **D** were 87.06 and 117.7 mm/h, respectively, but ligands **3e** and **3h** have values of 150 and 156 mm/h, respectively. Then, a faster coagulation-flocculation process is observed with these carboxyl-functionalized *bCCAs*. The Fig. S41 shows a diagram for the coagulation-flocculation process with ligand **3d** where it is observed that it takes only five minutes for the total flocs sedimentation and the height of the sediment is around 3 mm.

One key parameter for evaluating coagulant and flocculant performance in water treatment is the Turbiscan Stability Index (TSI), which considers destabilization kinetics and other phenomena. TSI values at 60 min are compared in Table 3 to determine the ligands which perform the best simultaneous removal of metal ions. Overall, the obtained TSI values (TSI $>$ 10) indicate that at the dose used all ligands promote a high destabilization [25,33]. Fig. 6A shows the TSI profiles for *N*-carboxyalkyl *bCCAs* **3a-3d** and for *N,N*-dihexyl *bCCA* **3i** for comparative purposes. It is notorious that carboxyl-functionalized ligands have an abrupt change in TSI with a great slope at the very first minutes which is not observed in the ligand **3i**, followed by a less pronounced second stage. This particular behavior was previously observed in pyridine-functionalized ligands **D** and **E** (Fig. 1) as a consequence of a fast complexation process between ligands and metal ions, where the terminal functional groups are involved in addition to the carbamoylcarboxylic functionality. Interestingly, ligand **3b** presents a multi-step destabilization process, a very abrupt change with a breaking

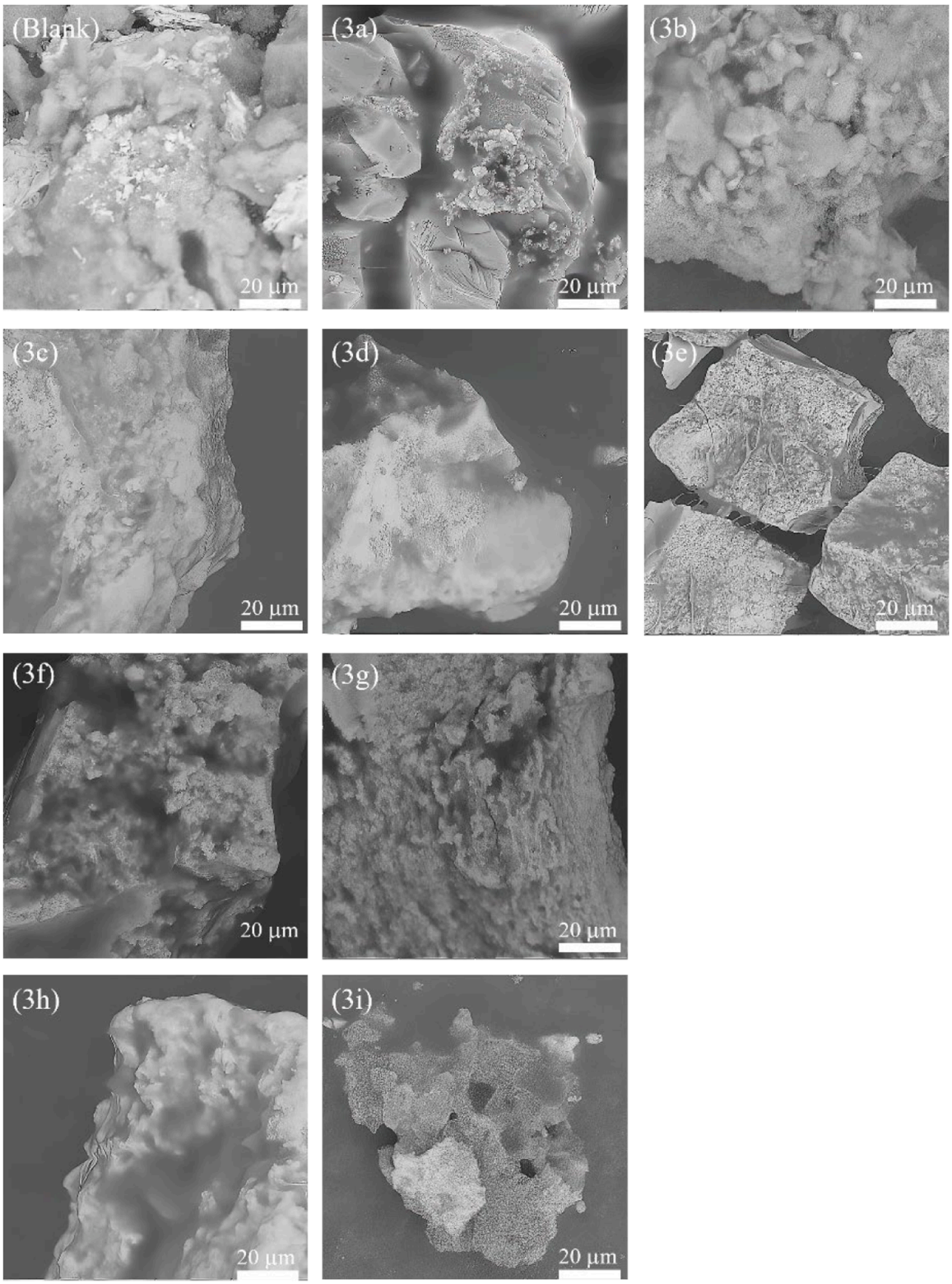

Fig. 7. SEM micrographs of dry flocs obtained in the model wastewater treatment with *bCCAs*.

point at 2 min, followed by a less pronounced change until 30 min, then occurs a second intense change that finishes at 50 min to finally reach the highest TSI value observed in these ligands. Fig. 6B shows the TSI profiles for *N*-carboxyaryl *bCCAs* **3e-3h** and for *N,N*-dibenzyl *bCCA* **3j** for comparative purposes. Once again, it is notorious the effect of the terminal carboxylic groups in the ligands over the instability process. Ligands **3e, 3f** and **3g** display the two stage instability process, while ligand **3h** shows a multi-step instability with several smooth slope changes. It is interesting that both non-carboxyl-functionalized ligands **3i** and **3j** present a slow instability process at the initial period of time, gradually increasing the TSI value until a moment where it abruptly increases. This behavior may be associated with a low complexation rate with these ligands followed by an aggregation process. In general, the instability process is faster with ligands **3a-3h** than ligands **D** and **E** [2,

25].

3.7. SEM analysis of recovered solids from a model wastewater treatment

The solids obtained in the treatment of model wastewater were recovered to analyze them by SEM. Fig. S42 shows the treatment by precipitation with hydroxide (blank sample) generates a turquoise color solid, while the solids obtained with carboxyl-functionalized *bCCAs* have a pale yellow color and the solid from the *N,N*-dihexyl *bCCA* has a pale green color. The flocs were separated and dried in order to obtain a series of solid samples (Fig. S43). SEM micrographs show the metal complex being imaged by retro-scattered electrons on the surface (Fig. 7). These electrons are capable of detecting variations in atomic number, indicating the presence of chemical elements with higher atomic weights through grayscale intensities. The contrast intensities are visible in all irregularly shaped particles, where the bright regions correspond to the heavy metals that have been removed [37,38]. These images show, from different perspectives, a very uniform distribution of the metallic elements along the particle's surface.

4. Conclusions

In conclusion, these newly synthesized carboxyl-functionalized *bCCAs* have shown promising results as coagulant and flocculant agents for the separation of hazardous metal ions from aqueous media. The interaction of these ligands with metal ions was successfully evaluated using UV-Vis spectroscopy and zeta potential analysis, demonstrating their capability to form metallic complexes with several metal ions. The presence of terminal carboxylic groups in these *bCCAs* ligands has not only enhanced the removal capacity of Pb^{2+}, but also other metal ions such as Ca^{2+} and Cd^{2+} are considerably removed, due to their versatile complexation capacity. In addition, these ligands display the best clarification kinetics and sedimentation ratios obtained for this type of ligands, achieving a very fast coagulation-flocculation process. Also, the formation of compact solids containing metal ions removed from wastewater was demonstrated by SEM analysis. All these characteristics point to these carboxyl-functionalized *bCCAs* ligands as potential candidates for metal ion removal in industrial applications. These results add to the existing knowledge of chelating agents for metal ion removal and open up avenues for the development of more efficient and easily synthesized compounds for environmental remediation purposes.

CRediT authorship contribution statement

Jorge Guzmán-Rasillo: Methodology, Investigation. **Adrián Ochoa-Terán:** Writing – original draft, Project administration, Formal analysis, Conceptualization. **Eduardo A. López-Maldonado:** Writing – review & editing, Project administration, Funding acquisition. **Sergio Pérez-Sicairos:** Resources, Investigation. **Balter Trujillo-Navarrete:** Resources, Investigation. **Luis Miguel López-Martínez:** Formal analysis. **José García-Elías:** Investigation. **Paul A. Sandoval-Hernandez:** Investigation. **Marisela Martínez Quiroz:** Resources, Investigation.

Declaration of competing interest

The authors declare that they have no known competing financial interests or personal relationships that could have appeared to influence the work reported in this paper.

Acknowledgements

The authors are grateful to the institutions involved in developing this research project. They also appreciate the Consejo Nacional de Humanidades, Ciencias y Tecnologías (CONAHCyT) for the financial support (Grant No. A1-S-38139) and the scholarship awarded to J. Guzmán-Rasillo to pursue postgraduate studies.

Supplementary materials

Supplementary material associated with this article can be found, in the online version, at doi:10.1016/j.molstruc.2025.142107.

Data availability

No data was used for the research described in the article.

References

[1] S. Mitra, A.J. Chakraborty, A.M. Tareq, T. Bin Emran, F. Nainu, A. Khusro, A. M. Idris, M.U. Khandaker, H. Osman, F.A. Alhumaydhi, J. Simal-Gandara, Impact of heavy metals on the environment and human health: novel therapeutic insights to counter the toxicity, J. King. Saud. Univ. Sci. 34 (2022) 101865, https://doi.org/10.1016/J.JKSUS.2022.101865.

[2] C. Zamora-Ledezma, D. Negrete-Bolagay, F. Figueroa, E. Zamora-Ledezma, M. Ni, F. Alexis, V.H. Guerrero, Heavy metal water pollution: a fresh look about hazards, novel and conventional remediation methods, Environ. Technol. Innov. 22 (2021) 101504, https://doi.org/10.1016/J.ETI.2021.101504.

[3] Water Security for All | Water, Sanitation and Hygiene, (n.d.). https://knowledge.unicef.org/wash/water-security-all (Accessed 17 July 2024).

[4] A. Mojiri, M.J.K. Bashir, Wastewater treatment: current and future techniques, Water 14 (2022) 448, https://doi.org/10.3390/W14030448.

[5] H. Abu Hassan, M. Hafizuddin Muhammad, N. 'Izzati Ismail, A review of biological drinking water treatment technologies for contaminants removal from polluted water resources, J. Water. Process. Eng. 33 (2020) 101035, https://doi.org/10.1016/j.jwpe.2019.101035.

[6] M.A. Al-Nuaim, A.A. Alwasiti, Z.Y. Shnain, The photocatalytic process in the treatment of polluted water, Chem. Pap. 77 (2023) 677–701, https://doi.org/10.1007/s11696-022-02468-7.

[7] R.M. El-taweel, N. Mohamed, K.A. Alrefaey, S. Husien, A.B. Abdel-Aziz, A.I. Salim, N.G. Mostafa, L.A. Said, I.S. Fahim, A.G. Radwan, A review of coagulation explaining its definition, mechanism, coagulant types, and optimization models; RSM, and ANN, Curr. Res. Green Sustain. Chem. 6 (2023) 100358, https://doi.org/10.1016/J.CRGSC.2023.100358.

[8] E.A. López-Maldonado, M.T. Oropeza-Guzman, J.L. Jurado-Baizaval, A. Ochoa-Terán, Coagulation–flocculation mechanisms in wastewater treatment plants through zeta potential measurements, J. Hazard. Mater. 279 (2014) 1–10, https://doi.org/10.1016/J.JHAZMAT.2014.06.025.

[9] K.Ogemdi Iwuozor, Prospects and challenges of using coagulation-flocculation method in the treatment of effluents, Adv. J. Chem. A 2 (2) (2019) 105–127, https://doi.org/10.29088/SAMI/AJCA.2019.2.105127.

[10] A.J. Hargreaves, P. Vale, J. Whelan, L. Alibardi, C. Constantino, G. Dotro, E. Cartmell, P. Campo, Coagulation–flocculation process with metal salts, synthetic polymers and biopolymers for the removal of trace metals (Cu, Pb, Ni, Zn) from municipal wastewater, Clean. Technol. Environ. Policy. 20 (2018) 393–402, https://doi.org/10.1007/S10098-017-1481-3/FIGURES/7.

[11] N.A.A. Qasem, R.H. Mohammed, D.U. Lawal, Removal of heavy metal ions from wastewater: a comprehensive and critical review, NPJ. Clean. Water. 1 (4) (2021) 1–15, https://doi.org/10.1038/s41545-021-00127-0.

[12] S.B. Pillai, N.V. Thombre, Coagulation, flocculation, and precipitation in water and used water purification, in: J. Lahnsteiner (Ed.), Handbook of Water and Used Water Purification, Springer, Cham, 2024, https://doi.org/10.1007/978-3-319-78000-9_63.

[13] S. Vasiljević, M. Vujić, J. Agbaba, S. Federici, S. Ducoli, R. Tomić, A. Tubić, Efficiency of coagulation/flocculation for the removal of complex mixture of textile fibers from water, Processes 11 (2023) 820, https://doi.org/10.3390/pr11030820.

[14] A.K. Badawi, R. Hassan, M. Farouk, S. Bakhoum, R.S. Salama, Optimizing the coagulation/flocculation process for the treatment of slaughterhouse and meat processing wastewater: experimental studies and pilot-scale proposal, Int. J. Environ. Sci. Technol. 21 (2024) 8431–8446, https://doi.org/10.1007/s13762-024-05591-y.

[15] G. Crini, E. Lichtfouse, Advantages and disadvantages of techniques used for wastewater treatment, Environ. Chem. Lett. 17 (2019) 145–155, https://doi.org/10.1007/S10311-018-0785-9/METRICS.

[16] E.A. López-Maldonado, O.G. Zavala García, K.C. Escobedo, M.T. Oropeza-Guzman, Evaluation of the chelating performance of biopolyelectrolyte green complexes (NIBPEGCs) for wastewater treatment from the metal finishing industry, J. Hazard. Mater. 335 (2017) 18–27, https://doi.org/10.1016/J.JHAZMAT.2017.04.020.

[17] M.H. Mohamed Noor, N. Ngadi, Ecotoxicological risk assessment on coagulation-flocculation in water/wastewater treatment: a systematic review, Environ. Sci. Pollut. Res. 31 (2024) 52631–52657, https://doi.org/10.1007/s11356-024-34700-0.

[18] R. Vidu, E. Matei, A.M. Predescu, B. Alhalaili, C. Pantilimon, C. Tarcea, C. Predescu, Removal of heavy metals from wastewaters: a challenge from current treatment methods to nanotechnology applications, Toxics 8 (2020) 101, https://doi.org/10.3390/TOXICS8040101.

[19] A. Roy, A.K. Jha, A. Kumar, T. Bhattacharya, S. Chakraborty, N.P. Raval, M. Kumar, Heavy metal pollution in indoor dust of residential, commercial, and industrial areas: a review of evolutionary trends, Air. Qual. Atmos. Health 17 (2024) 891–918, https://doi.org/10.1007/s11869-023-01478-y.

[20] E.A. López-Maldonado, H. Hernández-García, M.A.M. Zamudio-Aguilar, M. T. Oropeza-Guzmán, A. Ochoa-Terán, L.M. López-Martínez, M. Martinez-Quiroz, R. Valdez, A. Olivas, Chemical issues of coffee and Tule lignins as ecofriendly materials for the effective removal of hazardous metal ions contained in metal finishing wastewater, Chem. Eng. J.. 397 (2020) 125384, https://doi.org/10.1016/J.CEJ.2020.125384.

[21] P.B. Tchounwou, C.G. Yedjou, A.K. Patlolla, D.J. Sutton, Heavy metal toxicity and the environment, EXS 101 (2012) 133–164, https://doi.org/10.1007/978-3-7643-8340-4_6.

[22] F.N. Chowdhury, M.M. Rahman, Source and distribution of heavy metal and their effects on human health, in: N. Kumar (Ed.), Heavy Metal Toxicity. Environmental Science and Engineering, Springer, Cham, 2024, https://doi.org/10.1007/978-3-031-56642-4_3.

[23] E.A. Lopez-Maldonado, Y. Abdellaoui, M.H. Abu Elella, H.M. Abdallah, M. Pandey, E.T. Anthony, L. Ghimici, S. Álvarez-Torrellas, V. Pinos-Vélez, N.A. Oladoja, Innovative biopolyelectrolytes-based technologies for wastewater treatment, Int. J. Biol. Macromol. 273 (2024) 132895, https://doi.org/10.1016/J.IJBIOMAC.2024.132895.

[24] Y.C. López, G.A. Ortega, E. Reguera, Hazardous ions decontamination: from the element to the material, Chem. Eng. J. Adv. 11 (2022) 100297, https://doi.org/10.1016/j.ceja.2022.100297.

[25] M. Martínez-Quiroz, E.A. López-Maldonado, A. Ochoa-Terán, M.T. Oropeza-Guzman, G.E. Pina-Luis, J. Zeferino-Ramírez, Innovative uses of carbamoyl benzoic acids in coagulation-flocculation's processes of wastewater, Chem. Eng. J. Adv. 307 (2017) 981–988, https://doi.org/10.1016/J.CEJ.2016.09.011.

[26] M. Martínez-Quiroz, E.A. López-Maldonado, A. Ochoa-Terán, G.E. Pina-Luis, M. T. Oropeza-Guzman, Modification of chitosan with carbamoyl benzoic acids for testing its coagulant-flocculant and binding capacities in removal of metallic ions typically contained in plating wastewater, Chem. Eng. J. Adv. 332 (2018) 749–756, https://doi.org/10.1016/J.CEJ.2017.09.042.

[27] O.G.Z. García, M.T. Oropeza-Guzmán, W.M. Argüelles Monal, E.A. López-Maldonado, Design and mechanism of action of multifunctional BPE's with high performance in the separation of hazardous metal ions from polluted water Part I: Chitosan-poly(N-vinylcaprolactam) and its derivatives, Chem. Eng. J. Adv. 359 (2019) 840–851, https://doi.org/10.1016/J.CEJ.2018.11.134.

[28] R.M. El-taweel, N. Mohamed, K.A. Alrefaey, S. Husien, A.B. Abdel-Aziz, A.I. Salim, N.G. Mostafa, L.A. Said, I.S. Fahim, A.G. Radwan, A review of coagulation explaining its definition, mechanism, coagulant types, and optimization models; RSM, and ANN, Curr. Res. Green Sustain. Chem. 6 (2023) 100358, https://doi.org/10.1016/J.CRGSC.2023.100358.

[29] C. Zamora-Ledezma, D. Negrete-Bolagay, F. Figueroa, E. Zamora-Ledezma, M. Ni, F. Alexis, V.H. Guerrero, Heavy metal water pollution: A fresh look about hazards, novel and conventional remediation methods, Environ. Technol. Innov. 22 (2021) 101504, https://doi.org/10.1016/J.ETI.2021.101504.

[30] S. Mitra, A.J. Chakraborty, A.M. Tareq, T. Bin Emran, F. Nainu, A. Khusro, A. M. Idris, M.U. Khandaker, H. Osman, F.A. Alhumaydhi, J. Simal-Gandara, Impact of heavy metals on the environment and human health: Novel therapeutic insights to counter the toxicity, J. King. Saud. Univ. Sci. 34 (2022) 101865, https://doi.org/10.1016/J.JKSUS.2022.101865.

[31] M. Martínez-Quiroz, A. Ochoa-Terán, M. Aguilar-Martínez, J. García-Elías, H. Santacruz Ortega, V. Miranda-Soto, G. Pina-Luis, New fluorescent metal receptors based on 4,4′-carbonyl bis(carbamoylbenzoic) acid analogues with naphthalene fluorophore, Supramol. Chem. 29 (2017) 477–488, https://doi.org/10.1080/10610278.2016.1277585.

[32] A. Ochoa-Terán, J. Estrada-Manjarrez, M. Martínez-Quiroz, M.A. Landey-Álvarez, E. Alcántar Zavala, G. Pina-Luis, H. Santacruz Ortega, L.E. Gómez-Pineda, J. Z. Ramírez, D. Chávez, J. Montes Ávila, V. Labastida-Galván, M. Ordoñez, A novel and highly regioselective synthesis of new carbamoylcarboxylic acids from dianhydrides, Sci. World J. 2014 (2014) 725981, https://doi.org/10.1155/2014/725981.

[33] C.U. Montaño-Medina, L.M. Lopéz-Martínez, A. Ochoa-Terán, E.A. López-Maldonado, M.I. Salazar-Gastelum, B. Trujillo-Navarrete, S. Pérez-Sicairos, J. M. Cornejo-Bravo, New pyridyl and aniline-functionalized carbamoylcarboxylic acids for removal of metal ions from water by coagulation-flocculation process, Chem. Eng. J. Adv. 451 (2023) 138396, https://doi.org/10.1016/J.CEJ.2022.138396.

[34] C.L. Castro-Riquelme, E.A. López-Maldonado, A. Ochoa-Terán, E. Alcántar-Zavala, B. Trujillo-Navarrete, S. Pérez-Sicairos, V. Miranda-Soto, A. Zizumbo-López, Chitosan-carbamoylcarboxylic acid grafted polymers for removal of metal ions in wastewater, Chem. Eng. J. Adv. 456 (2023) 141034, https://doi.org/10.1016/J.CEJ.2022.141034.

[35] E.A.L. Maldonado, A. Ochoa-Terán, M.T. Oropeza Guzmán, A multiparameter colloidal titrations for the determination of cationic polyelectrolytes, J. Environ. Prot. (2012) 1559–1570, https://doi.org/10.4236/JEP.2012.311172.

[36] P. Thordarson, Determining association constants from titration experiments in supramolecular chemistry, Chem. Soc. Rev. 40 (2011) 1305–1323, https://doi.org/10.1039/C0CS00062K.

[37] T.W. Napporn, C. Canaff, E. Bere, V. Hacker, Characterization methods for components and materials. Fuel Cells and Hydrogen: From Fundamentals to Applied Research, 2018, pp. 155–173, https://doi.org/10.1016/B978-0-12-811459-9.00008-6.

[38] M. Ohring, L. Kasprzak, Characterization and failure analysis of materials and devices, Reliability and Failure of Electronic Materials and Devices (2015) 611–664, https://doi.org/10.1016/B978-0-12-088574-9.00011-2.